referred to as $\mu_0$, which increases as $R_1$ increases: $\mu_0 = 3{\cdot}3$, $3{\cdot}9$, $4{\cdot}5$ and $5{\cdot}0$ for $R_1 = 10, 12, 14$ and 16 bits, respectively.

For a specific value of $R_1$, as $\mu$ increases from $\mu_0$, $\Delta$ increases rapidly up to a maximum value $\Delta = \Delta_{max}$ which corresponds to a value of $\mu = \mu_{opt}$. Owing to the steepness of $\Delta(\mu)$ in the vicinity of $\mu_0$, $(\mu_{opt} - \mu_0)/\mu_0$ is only a few percent. For the values of $R_1$ considered here, $\Delta_{max}$ is bounded by $2 \leq \Delta_{max} \leq 3$. Thus a significant reduction of $R_2$ is obtained by clipping, resulting in a reduced implementation complexity in the A/D–D/A convertors. This is especially valuable at high clock rates. It is also important to note from Fig. 2 that the range of $\mu$ for which $\Delta$ is larger than a specific value decreases as $R_1$ increases. This may turn the advantage to frequency division multiplexed (FDM) ADSL systems compared to echo cancellation (EC) systems ($R_1$ is larger for EC-ADSL than for FDM-ADSL).

As $\mu$ further increases from $\mu_{opt}$, the increase of the amplitude dynamic range $(2 \,.\, A_{Clip})$ dominates over the decrease of $(S/N)_{Q_2}$ which results in the negative slope of the $\Delta$ curve in Fig. 2. When $A_{Clip}$ approaches $A_{max}$, $(S/N)_{Clip} \to \infty$ and, therefore, all curves in Fig. 2 converge for large $\mu$.

The above analysis considers identical QAM constellation sizes for all subchannels in the DMT signal. However, within DMT–ADSL systems, the QAM size may vary by a large factor from subchannel to subchannel. Nevertheless, preliminary simulations have shown that this only leads to minor changes in the results presented here. Results of these simulations will be published in a separate paper.

In summary, we have obtained an analytical expression for the gain of the number of bits required for the A/D–D/A convertors within ADSL transceivers when the amplitude of a DMT signal is clipped to a predetermined level. The results show that a significant reduction of the A/D–D/A precision can be obtained by clipping while keeping the same signal-to-noise ratio as when clipping is not applied.

*Acknowledgments:* Discussions with M. Moeneclaey and J. Cioffi were greatly appreciated.

 *2nd June 1993*

D. J. G. Mestdagh, P. M. P. Spruyt and B. Biran (*Alcatel-Bell, Research Center, 1, Francis Wellesplein, B-2018 Antwerp, Belgium*)

**References**

1 KALET, I.: 'The multitone channel', *IEEE Trans.*, 1989, **COM-37**, (2), pp. 119–124
2 FELLER, W.: 'An introduction to probability theory and its applications, Vol. II' (J. Wiley & Sons, New York, 1971), 2nd edn.
3 PROAKIS, J. G.: 'Digital communications' (McGraw-Hill, New York, 1989), 2nd edn.
4 SALEH, A. A. M.: 'Fundamental limit on number of channels in subcarrier multiplexed lightwave CATV systems', *Electron. Lett.*, 1989, **25**, (12), pp. 776–777

## LOW-VOLTAGE LOW-POWER CONTROLLED ATTENUATOR FOR HEARING AIDS

A. van Staveren and A. H. M. van Roermund

*Indexing terms: Filters, Biomedical electronics*

A novel controllable current attenuator for completely integrable hearing aids is presented. Much attention has been paid to obtaining good signal to noise ratio and low distortion. The attenuation can be controlled logarithmically. The attenuator is designed for a supply voltage of 1–1·3 V and can be used with both symmetric and asymmetric signal paths. The maximal supply current is 50 μA.

*Introduction:* Many people with hearing impairments need a hearing aid with a (controllable) highpass filter [1]. A new generation of hearing aids has recently been developed in our laboratory [2, 3], in which all capacitors can be integrated and which contains a controllable highpass filter. Fig. 1 shows a block diagram of the hearing aid.

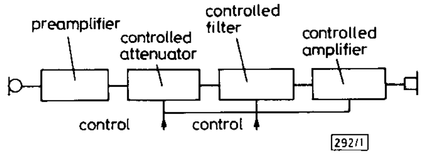


**Fig. 1** *Block diagram of new generation of hearing aids*

To make the integration of all the capacitors possible, the filter must be biased at very low currents ($\tau = C/g_m$). Further, for optimal use of the dynamic range the input current for the filter must be 25 nA [2]. The output current of the preamplifier can vary between 40 nA and 10 μA (peak value) [3]. Therefore a controlled attenuator is needed with a control range of −4 to −52 dB. In line with the usual specifications for hearing aids, the minimal required signal to noise ratio is 50 dB and the distortion must be less than 5%. A variant of the beta-immune type-'A' cell [5] has been chosen as the basic configuration (Fig. 2).

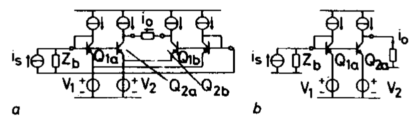


**Fig. 2** *Variant of beta-immune type-'A' cell*
*a* Symmetric circuit
*b* Asymmetric circuit

*Beta-immune type-'A' cell:* The magnitude of the transfer can be set by the voltage sources $V_1$ and $V_2$. For both circuits: $V_1 + V_{be1} = V_2 + V_{be2}$, where $V_{be1}$ and $V_{be2}$ are the base–emitter voltages of $Q_1$ and $Q_2$. If the transistors have the same emitter area and the transistor equation is given by $I_c = I_s \exp(V_{be}/V_T)$, the current transfer $A_i$ of the input signal current $i_s$ to the output current $i_o$ yields

$$20 \log (A_i) = 20 \log \{\exp [(V_1 - V_2)/V_T]\} \simeq 335(V_1 - V_2) \text{ [dB]} \quad (1)$$

where $V_T$ (the thermal voltage $kT/q$) is $\sim$26 mV at $T = 300$ K and $V_1$ and $V_2$ are in Volts. Each extra difference of the voltages $V_1$ and $V_2$ of $-(1/335)V = -3$ mV means an extra attenuation of 1 dB. The attenuation can simply be controlled logarithmically. Because the circuit is used as an attenuator only, the source $V_1$ is chosen as 0 V. The attenuation $N(>1)$ can then be defined as

$$N = (i_o/i_s)^{-1} = (I_{C2}/I_{C1})^{-1} \quad (2)$$

where $I_{C1}$ is the collector current of $Q_{1a}$ and $Q_{1b}$, and $I_{C2}$ the collector current of $Q_{2a}$ and $Q_{2b}$.

*Distortion characteristics:* Here we will only examine the distortion properties of the asymmetric circuit because those of the symmetric circuit are better (compensation of the even order harmonics). At minimal attenuation the input impedance of the asymmetric attenuator is of the order of magnitude of the source impedance. Owing to the input signal variation, the input impedance will vary strongly. This leads to highly signal-dependent current splitting, resulting in much distortion.

*Reduction of the distortion by an extra amplifier:* By using an extra amplifier the distortion lowers considerably. Fig. 3 shows the asymmetric attenuator with the extra amplifier ($Q_A$, $Q_B$, $Q_C$ and $Q_D$).

The input impedance $r_i$ of the asymmetric attenuator is given by

$$r_i = \frac{r_{\pi A}}{1 + \frac{1}{2}\beta_1\beta_A \cdot r_{\pi 2}/(r_{\pi 1} + r_{\pi 2})} \quad [\Omega] \quad (3)$$

where $\beta_1$ and $\beta_A$ are the current gain factors of $Q_{1a,b}$ and $Q_A$, respectively, and $r_\pi = \beta/g_m$. The input impedance is now very low. Hence, the current splitting at the input will be much less signal dependent, so the distortion is reduced.

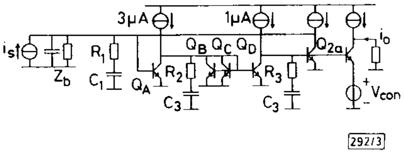


**Fig. 3** *Asymmetric attenuator with extra amplifier*

*Noise characteristics:* To obtain the noise level, we transform all the noise sources to the output with the transformation techniques as described in Reference 6. Only the contributions of the base shot noise and collector shot noise are relevant. If $\beta \gg 1$ the noise spectrum $S(i_{out})$ is given by

$$S(i_{out}) = 2qI_{C2}(1 + 1/N) + 2qI_{BA}/N^2 \qquad [A^2/Hz] \quad (4)$$

where $I_{C2}$ is the collector current of $Q_2$ and $I_{BA}$ is the base current of $Q_A$. For the symmetric attenuator the noise power spectrum will be halved compared with that of the asymmetric attenuator [6], and the signal current will be doubled. Therefore the signal to noise ratio increases by 9 dB.

As the biasing current of $Q_1$ can be chosen small without enlarging the distortion considerably, the noise contribution can be minimised by choosing the biasing currents of $Q_1$ and $Q_2$ as small as possible. An adequate choice for the biasing currents is 1·2 times the maximal amplitude of the signal. Thus $I_{C2} = 30$ nA and $I_{C1}$ varies as a function of the attenuation from 48 nA to 12 µA.

*Frequency behaviour of the extra amplifier:* The loop ($Q_{1a}$, $Q_A$, $Q_B$, $Q_C$ and $Q_D$) contains three poles. One pole is contributed by $Q_A$, one by $Q_B$, $Q_C$, $Q_D$ and one by $Q_{1a}$. The latter strongly depends on the control voltage $V_{con}$. The high-frequency behaviour is stabilised by pole-zero cancellation [7] by means of $R_1 - C_1$, $R_2 - C_2$ and $R_3 - C_3$.

*Controllable voltage source:* With the voltage source $V_{con}$ the attenuation of the circuit can be controlled. Its output impedance must be low so that the contribution to the distortion can be neglected. The voltage follower of Fig. 4 has been chosen for three reasons. First, the level shift at the input ($Q_{V1}$ and $Q_{V2}$) is almost independent of the output voltage $V_{con}$.

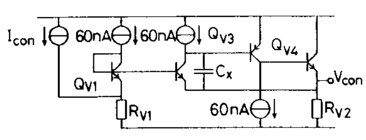


**Fig. 4** *Controllable voltage source*

Secondly, the follower has a very low output impedance and finally, the high-frequency behaviour is easy to stabilise.

The four transistors are biased at 60 nA, furthermore the bias current of $Q_{V4}$ is dependent on $V_{con}$. For biasing reasons the values of $R_{V1}$ and $R_{V2}$ are chosen as 75 and 50 kΩ, respectively. The loop gain of the voltage source contains two dominant poles: one pole due to $Q_{V3}$ and one due to $Q_{V4}$. With capacitor $C_x$ the high-frequency behaviour is stabilised. The influence of $C_x$ is enlarged by a factor 12 due to the Miller effect [6]. For $C_x$ a value of 10 pF is chosen. The voltage source is controlled by a current $I_{con}$ in the range 0–1·92 µA. The corresponding output voltage range extends from 12 to 156 mV.

*Biasing:* The circuit is biased by a common-mode loop (Fig. 5). In this loop the shunt stage ($Q_s$) has two functions. First, it makes the loop gain independent of the attenuation factor and secondly it stabilises (together with $C_s$) the common-mode frequency behaviour of the extra amplifiers. For the shunt resistor an amount of 200 kΩ is chosen (power efficiency). The high-frequency behaviour of the common-mode is stabilised by pole-zero cancellation.

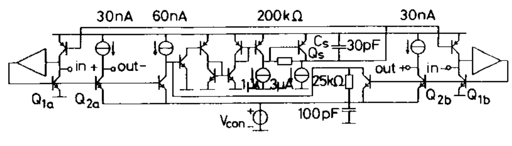


**Fig. 5** *Attenuator with common-mode loop*

When the bias sources of the output transistors are replaced by a current mirror, at the cost of an extra 3 dB noise, the attenuator can be used in an asymmetric signal path.

*Realisation:* The circuit has been realised in a fully-custom process of the Delft Institute for Microelectronics and Submicron Technology (DIMES) [8]. For the components used for the pole-zero cancellation (Fig. 3) the following values have been chosen: $R_1 = 5$ kΩ, $C_1 = 15$ pF, $R_2 = 8$ kΩ, $C_2 = 15$ pF, $R_3 = 250$ kΩ and $C_3 = 10$ pF. The attenuation as a function of frequency with parameter $V_{con}$ is shown in Fig. 6.

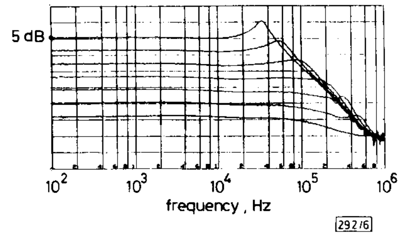


**Fig. 6** *Attenuation as function of frequency with parameter $V_{con}$*

The signal to noise ratio is 62 and 56 dB for the symmetric and the asymmetric signal path, respectively. With a source impedance of 1 MΩ//1 pF in the asymmetric situation the distortion is 0·5%. In the symmetric case the distortion is 0·2%, with source impedances of 1 MΩ//1 pF to ground at each input. The maximum measured current drain is 48 µA.

*Acknowledgments:* The authors would like to thank DIMES for processing the chip.


*7th June 1993*

A. van Staveren and A. H. M. van Roermund (*Delft University of Technology, Department of Electrical Engineering, Electronics Research Laboratory, Mekelweg, 4, 2628 CD Delft, The Netherlands*)

**References**

1 VILLCHUR, E.: 'Signal processing to improve speech intelligibility in perceptive deafness', *J. Acoust. Soc. Am.*, June 1972, **53**, pp. 1646–1657

2 SERDIJN, W. A.: 'A low-voltage low-power current-mode high-pass leapfrog filter'. Analog Integrated Circuits and Signal Processing 3, 1993, pp. 105–112

3 PLUYGERS, A. C.: 'A novel microphone preamplifier for use in hearing aids'. Analog Integrated Circuits and Signal Processing 3, 1993, pp. 113–118

4 VAN DER WOERD, A. C.: 'Analog circuits for a single-chip infra-red controlled hearing aid'. Analog Integrated Circuits and Signal Processing 3, 1993, pp. 91–103

5 TOUMAZOU, C., LIDGEY, F. J., and HAIGH, D. G. (Eds.): 'Analogue IC design: the current-mode approach' (Peter Peregrinus Ltd., London, 1990), Chap. 2

6 DAVIDSE, J.: 'Analog electronic circuit design' (Prentice-Hall International Ltd., 1991)

7 NORDHOLT, E. H.: 'Design of high performance negative feedback amplifiers' (Elsevier Scientific Publishing Company, Amsterdam, 1983)

8 NANVER, L K., GOUDENA, E. J. G., and VAN ZEIGL, H. W.: 'DIMES-01, a baseline BIFET process for smart sensor experimentation', *Sens. & Actuators*, 1993, **36**, (2), pp. 139–147